Cation-Dependent Formation of Superstructures by One-Pot Self-Organization of Hydrogen-Bonded Nickel Complexes**

Makoto Tadokoro,* Kiyoshi Isobe, Hidehiro Uekusa, Yuji Ohashi, Jiro Toyoda, Koji Tashiro, and Kazuhiro Nakasuji*

The unique strength, directionality, and complementarity of noncovalent interactions such as hydrogen bonding and coordination bonding play a central role in the creation of a variety of molecular architectures for molecular self-assembly and recognition in chemical, physical, and biological sciences.[1, 2] The building blocks possessing such noncovalent interaction sites can produce one-, two-, and three-dimensional molecular arrangements with long-range order.[3–5] Control of such multidimensional molecular arrangements is essential for progressing crystal engineering and in constructing the desired molecular-based materials.[6–8] We have designed a new anionic building block, a tris(biimidazolato)-nickel(II) complex, in which the three strong, π-conjugated biimidazolate ligands each provide one complementary hydrogen-bonding site. We now report the construction of four types of hydrogen-bonded and coordination-bonded molecular architectures of nickel(II) ions, biimidazolate ligands, and counter cations.

Since 2,2′-biimidazole (H_2bim) is a bidentate chelating ligand with multiple proton-donor sites, it can coordinate to a transition metal in three reversible protonated and deprotonated modes: neutral (H_2bim), monoanionic ($Hbim^{-1}$), and dianionic (bim^{-2}).[9] The mono-deprotonated ligand ($Hbim^{-1}$) can form both a complementary binary NH···N-type hydrogen bond and a coordination bond with metal ions (see structure **A**).[10]

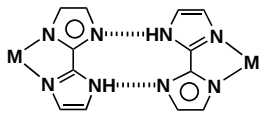

A

In this study, we have found that simple one-pot procedures[11] of mixing the nickel(II) ions, $Hbim^{-1}$, and counter cations produces four types of hydrogen-bonded crystals (**1**–**4**) based on arrangements of the $[Ni(Hbim)_3]^-$ building blocks (Figure 1). Figures 2 and 3 show the schematic drawings and crystal structures of the four types of molecular arrangements.

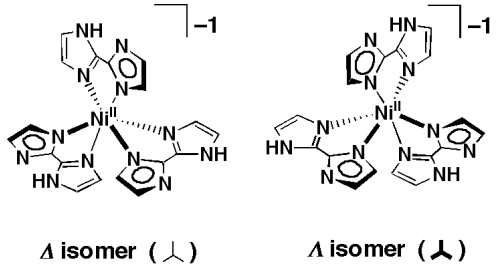

Figure 1. Λ and Δ isomers of the building block $[Ni(Hbim)_3]^-$.

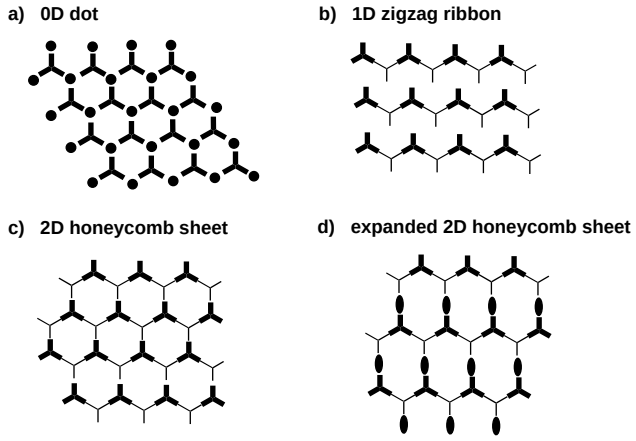

Figure 2. Schematic representations of the hydrogen-bonded networks of $[Ni(Hbim)_3]^-$ building blocks for **1**–**4** (a–d). Water molecules (●) and free 2,2′-biimidazole (⬮) also function as intermediate spacers.

As a common feature, all the structures contain the anionic building block $[Ni(Hbim)_3]^-$, in which the central Ni^{II} atom is coordinated by three bidentate $Hbim^-$ ligands through the lone pairs of the imine nitrogen atoms in the imidazole rings. The Ni–N bond lengths are in the range of 1.96(3)–2.19(2) Å. The building block has approximate D_3 symmetry; both the Δ and Λ isomers are illustrated in Figure 1.

Structure **1**[12a] contains tetramethylammonium as the counter cation (Figures 2a, 3a). Although there is no hydrogen bonding between the ligands of the $[Ni(Hbim)_3]^-$ building blocks, the units are connected by hydrogen bonding through water molecules to make a sheet arrangement along the *ab* plane (Figure 2a): The length of the hydrogen bonds between the oxygen atoms of the water molecules and the nitrogen atoms of the $Hbim^-$ ligands are 2.753(4) and 2.756(4) Å. The water molecules themselves form a 1D columnar structure along the *c* axis. A single sheet consists of only one of the two optical isomers (Δ or Λ). The whole structure is formed by an alternate stacking of the Δ and Λ sheets along the *c* axis, and the NMe_4^+ counter cations occupy the cavity formed between three $[Ni(Hbim)_3]^-$ building blocks in a sheet.

Structure **2**[12b] contains tetra(*n*-propyl)ammonium as the counter cation (Figures 2b, 3b). Of the three hydrogen-bonding sites in the building block, the one oriented along the *b* axis is blocked by hydrogen bonding with a methanol molecule. The other two sites are linked by complementary

[*] Prof. M. Tadokoro, Prof. K. Isobe
Graduate School of Science
Osaka City University
Sumiyoshi-ku, Osaka 558-8585 (Japan)
Fax: (+81) 6-605-2522
E-mail: tadokoro@sci.osaka-cu.ac.jp
Prof. K. Nakasuji, Dr. J. Toyoda, Prof. K. Tashiro
Graduate School of Science
Osaka University
Toyonaka, Osaka 560-0043 (Japan)
Fax: (+81) 6-850-5392
E-mail: nakasuji@chem.sci.osaka-u.ac.jp
Dr. H. Uekusa, Prof. Y. Ohashi
Faculty of Science
Tokyo Institute of Technology O-okayama (Japan)

[**] This work was supported by a Grant-in-Aid for Scientific Research (no. 10146103) on Priority Areas from the Ministry of Education, Science and Culture, Japan. The authors thank the Analytical Center, Osaka City University, for the use of a four-circle single-crystal X-ray diffractometer and for an elemental analysis.

  1433-7851/99/3801-0095 $ 17.50+.50/0

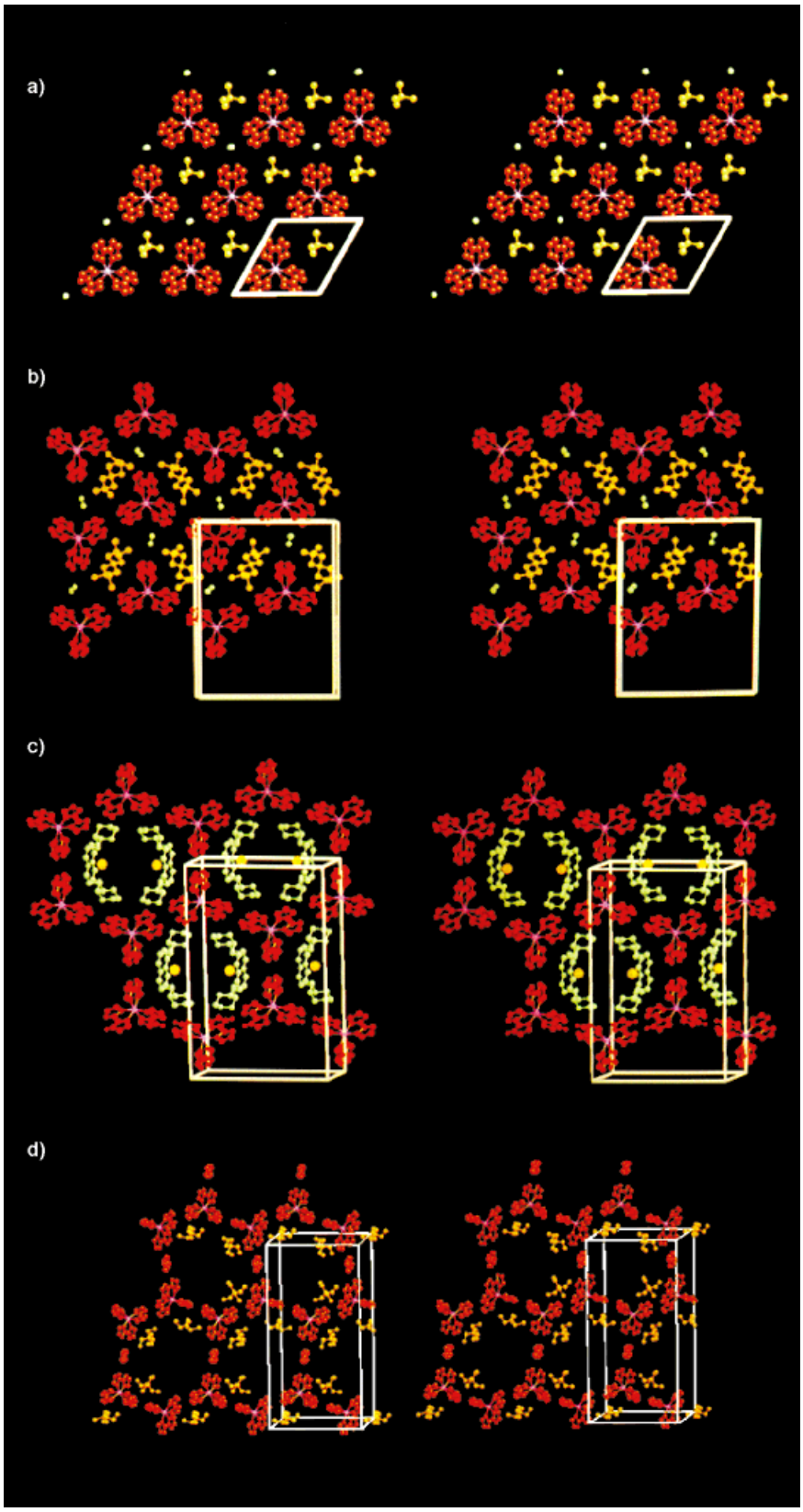

Figure 3. Arrangement of the $[Ni(Hbim)_3]^-$ building blocks in the crystal structures (stereoviews): a) "Zero-dimensional" dot structure without complementary hydrogen bonds between the ligands in $[NMe_4][Ni(Hbim)_3]$ (**1**), as viewed along the *c* axis. b) One-dimensional zigzag ribbon structures in $[NnPr_4][Ni(Hbim)_3]$ (**2**), as viewed along the *c* axis. c) Double-channel structures built up by two-dimensional honeycomb sheets in [K(DCH[18]crown-6)][$Ni(Hbim)_3$] (**3**). The inner channels (yellow) are constructed by K^+–crown ether complexes, and the outer channels (red) are constructed by the $[Ni(Hbim)_3]^-$ building blocks to form a microporous crystal. d) Two-dimensional expanded honeycomb sheet structure in $[NEt_4]_2[\{Ni(Hbim)_3\}_2(H_2bim)]$ (**4**), as viewed along the *a* axis. The free neutral H_2bim ligands connect zigzag ribbons through complementary hydrogen bonds to form an expanded sheet structure along the *bc* plane.

binary NH···N hydrogen bonds to produce a 1D zigzag ribbon structure along the *a* axis (Figure 2b); the ribbon is made up of alternating Δ and Λ isomers of the building block. The N···N distances of intermolecular hydrogen bonds are 2.70(2), 2.76(3), 2.89(2), and 2.91(1) Å. The $NnPr_4^+$ counter cations occupy the cavity formed between the ribbons.

Structure **3**[12c] contains potassium *cis-syn-cis*-dicyclohexano-[18]crown-6 ($[K(DCH[18]crown\text{-}6)]^+$) as the counter cation (Figures 2c, 3c). The characteristic feature is that **3** has a microporous structure with a double-channel system (Figure 3c). All three ligands of the $[Ni(Hbim)_3]^-$ building blocks form complementary intermolecular hydrogen bonds. Interactions of two of the hydrogen-bonding sites result in a 1D hydrogen-bonded zigzag ribbon as for **2**. Then, the ribbons are connected to each other through the remaining hydrogen-bonding site to form 2D honeycomb sheets along the *ab* plane in which each hexagon is made up of alternating Δ and Λ optical isomers of $[Ni(Hbim)_3]^-$ (Figure 2c). The sheets are stacked along the *c* axis in such a way that $[Ni(Hbim)_3]^-$ units of the same chirality are above each other in the outer channels formed (Figure 4a). The N···N distances of intermolecular hydrogen bonds are 2.737(9) and 2.74(1) Å. The inner channels are formed by stacking of two $[K(DCH[18]crown\text{-}6)]^+$ cations facing each other along the *c* axis. The channel contains methanol and water molecules that are involved in hydrogen bonding.

Structure **4**[12d] contains tetraethylammonium as the counter cation (Figures 2d, 3d). This crystal structure shows an unprecedented example of a 3D supra-cross-catenated self-organization based on hydrogen-bonded networks of the anionic $[Ni(Hbim)_3]^-$ building blocks (Figures 4b, c). The crystal has four structural characteristics. First, there is a 1D zigzag ribbon

  1433-7851/99/3801-0096 $ 17.50+.50/0

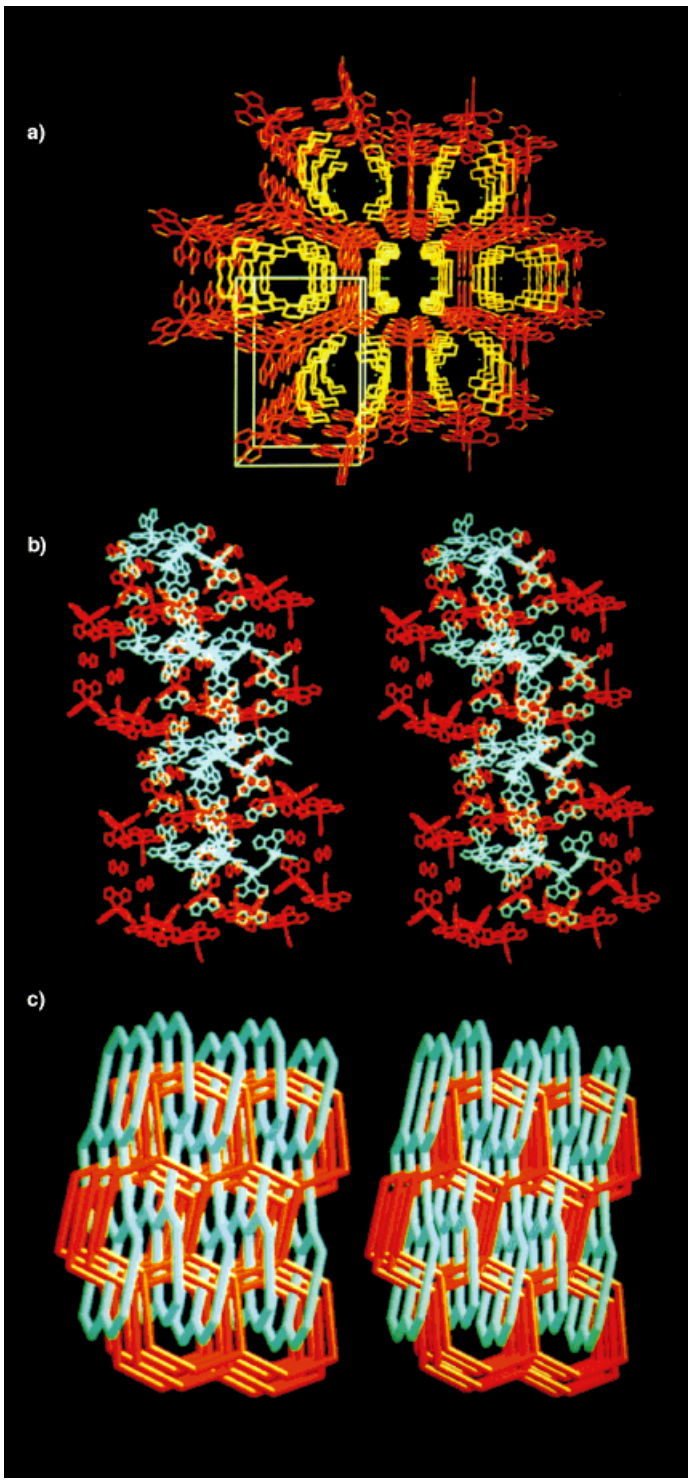

Figure 4. Representations of the final crystal structures for **3** and **4**. a) A perspective view of the microporous structure with a double channel formed by $[Ni(Hbim)_3]^-$ building blocks and K^+–crown ether complexes for **3**. b) A part of the polycatenate network for **4** (stereoview) c) Schematic drawing of the polycatenate network for **4** (stereoview): The straight lines represent the distance between nickel ions in two $[Ni(Hbim)_3]^-$ building blocks connected by hydrogen bonds. A double-interlocking polycatenate structure is formed by two sets of stacked honeycomb sheets (red and blue) that are perpendicular to each other.

arrangement of the anions similar to that in **2**; the distances of hydrogen bonds between the building blocks are 2.77(1), 2.78(1), 2.82(1), and 2.84(1) Å. Second, free neutral H_2bim ligands connect the 1D ribbons by complementary hydrogen bonding to form an expanded 2D honeycomb sheet along the *bc* plane; the N···N distances of the hydrogen bonds are 2.70(1), 2.76(1), and 2.84(1), 2.88(1) Å. Third, two sets of honeycomb sheets that are perpendicular to each other interpenetrate to construct a double-interlocking catenate structure. Finally, the catenated structure is arranged in 3D to form an infinite interlocking cross-catenated structure (Figure 4c).

The production of the four types of molecular architectures by the one-pot molecular self-organization of the anionic building blocks evolves from three fundamental factors: 1) the presence of three complementary binary hydrogen-bonding sites, 2) the occurence of Δ and Λ optical isomers of the anionic nickel building blocks, and 3) the identity of the counter cations. Therefore, our results suggest that the mode of self-organization can be controlled by varying the kind of counter cation, although at this stage the cation specificity is difficult to predict. With a systematic approach, we have succeeded in the organization of $[Ni(Hbim)_3]^-$ building blocks to microporous crystals of type **3** with double channels and crystals of type **4** with double-interlocking chains as polycatenate structures. These created crystals are involved in the construction of organic zeolites[13] and superstructures for supramolecular chemistry.[14] Our further study will be aimed at finding the mutual relationship between the building blocks and the kinds or shapes of counter cations for hydrogen-bonded superstructures. Thus, the cations play an important role in the prediction of crystal structures and the rationalization of the crystal structure engineering in this systems. In addition, the introduction of paramagnetic metal ions and transition metal chromophores into the system of the hydrogen-bonding extended arrays may lead to a new material with interesting magnetic and electronic properties.

Experimental Section

1: A suspension of H_2bim (0.4 g, 3 mmol) and $Me_4NOH \cdot 5H_2O$ (0.42 g, 2.2 mmol) in methanol (60 mL) was added to a 28% NaOMe solution in methanol (5 mL) and heated under reflux until the ligand had dissolved. A solution of $Ni(ClO_4) \cdot 6H_2O$ (0.36 g, 1 mmol) in methanol (40 mL) was added dropwise, and the mixture was heated under reflux for 15 min. The insoluble components were removed by filtration, and the filtrate was allowed to stand at room temperature. After renewed filtration of white precipitate, blue prisms were obtained from the filtrate after several weeks. Elemental analysis calcd for $[NMe_4][Ni(Hbim)_3] \cdot 2H_2O$ ($C_{22}H_{31}N_{13}NiO_2$): C 46.50, H 5.50, N 32.04; found: C 46.98, H 5.09, N 32.36; IR (KBr): $\tilde{\nu}$ = 2620 (br, ν(NH)), 1899 cm^{-1}(br, 2γ(NH)).

Crystals **2**–**4** were obtained by a method similar to that of **1**, except that different counter cations were used. **2**: Elemental analysis calcd for $[NnPr_4][Ni(Hbim)_3] \cdot MeOH$ ($C_{31}H_{47}N_{13}NiO$): C 55.04, H 7.00, N 26.92; found: C 54.51, H 6.53, N 27.34; IR (KBr): $\tilde{\nu}$ = 2844 (br, ν(NH)), 1912 cm^{-1}(br, 2γ(NH)). **3**: Elemental analysis calcd for $[K(DCH[18]crown\text{-}6)][Ni(Hbim)_3] \cdot 0.5H_2O$ ($C_{38}H_{52}N_{12}KNiO_{6.5}$): C 50.90, H 6.07, N 18.74; found: C 50.85, H 5.86, N 18.77 (sample dried under vacuum for 6 h at 100 °C); IR (KBr): $\tilde{\nu}$ = 2513 (br, ν(NH)), 1902 cm^{-1} (br, 2γ(NH)). **4**: Elemental analysis calcd for $[NEt_4]_2[\{Ni(Hbim)_3\}_2(H_2bim)] \cdot MeOH \cdot H_2O$ ($C_{59}H_{82}N_{30}Ni_2O_2$): C 52.07, H 6.07, N 30.88; found: C 52.02, H 6.16, N 30.32; IR (KBr): $\tilde{\nu}$ = 2811 (br, ν(NH)), 1912 cm^{-1} (br, 2γ(NH)).

Received: July 27, 1998 [Z12213IE]
German version: *Angew. Chem.* **1999**, *111*, 102–106

  1433-7851/99/3801-0097 $ 17.50+.50/0

Keywords: crystal engineering · hydrogen bonds · N ligands · nickel · supramolecular chemistry

[1] J.-M. Lehn, *Supramolecular Chemistry*, VCH, Weinheim, **1995**.
[2] a) G. M. Whitesides, J. P. Mathias, C. T. Seto, *Science* **1991**, *254*, 1312 – 1319; b) J. Rebek, Jr., *Angew. Chem.* **1990**, *102*, 261 – 272; *Angew. Chem. Int. Ed. Engl.* **1990**, *29*, 245 – 255.
[3] a) S. Subramanian, M. J. Zaworotko, *Coord. Chem. Rev.* **1994**, *137*, 357 – 401; b) O. Ermer, *J. Am. Chem. Soc.* **1988**, *110*, 3747 – 3754.
[4] a) M. C. Etter, *Acc. Chem. Res.* **1990**, *23*, 120 – 126; b) C. B. Aakeröy, K. R. Seddon, *Chem. Soc. Rev.* **1993**, *26*, 397 – 407.
[5] I. Weissbuch, R. P. Biro, M. Lahav, L. Leiserowitz, *Acta Crystallogr. Sect. B* **1995**, *51*, 115 – 148.
[6] a) G. R. Desiraju, *Crystal Engineering: The Design of Organic Solids*, Elsevier, Amsterdam, **1989**; b) G. R. Desiraju, *Angew. Chem.* **1995**, *107*, 2541 – 2558; *Angew. Chem. Int. Ed. Engl.* **1995**, *34*, 2311 – 2327.
[7] J. C. MacDonald, G. M. Whitesides, *Chem. Rev.* **1994**, *94*, 2383 – 2420.
[8] a) M. J. Zaworotko, *Chem. Soc. Rev.* **1994**, *137*, 283 – 288; b) A. D. Burrows, C.-W. Chan, M. M. Chowdhry, J. E. McGrady, D. M. P. Mingos, *Chem. Soc. Rev.* **1995**, *138*, 329 – 339.
[9] S. W. Kaiser, R. B. Saillant, W. M. Butler, P. G. Rasmussen, *Inorg. Chem.* **1976**, *15*, 2681 – 2687.
[10] M. Tadokoro, J. Toyoda, K. Isobe, T. Itoh, A. Miyazaki, T. Enoki, K. Nakasuji, *Chem. Lett.* **1995**, 613 – 614.
[11] M. M. Chowdhry, D. M. P. Mingos, A. J. P. White, D. J. Williams, *Chem. Commun.* **1996**, 899 – 900.
[12] Crystal structure determinantions. General: Crystallographic data (excluding structure factors) for the structures reported in this paper have been deposited with the Cambridge Crystallographic Data Centre as supplementary publication nos. CCDC-103363 – 103366. Copies of the data can be obtained free of charge on application to CCDC, 12 Union Road, Cambridge CB2 1EZ, UK (fax: (+44) 1223-336-033; e-mail: deposit@ccdc.cam.ac.uk). a) Crystal data for **1**: $C_{22}H_{31}O_2N_{13}Ni_2$, $M_r = 568.27$, trigonal, space group $P\bar{3}$ (no. 147), $a = 11.167(2)$, $c = 13.206(4)$ Å, $V = 1426.1(3)$ Å^3, $Z = 2$, $\rho_{calcd} = 1.323$ g cm^{-3}, $F(000) = 596$, 106 parameters; $R_1 = 0.060$, $R_w = 0.080$, GOF = 1.55 for all 1613 data ($I > 3\sigma(I)$); max./min. residual electron density: 0.79/ – 0.36 e Å^{-3}. Diffractometer: Rigaku AFC5R; $\mu(Mo_{K\alpha}) = 7.24$ cm^{-1}; Lp correction; 3094 reflections collected; the structure was solved with the program PATTY, and refined with the program DIRDIF92; reflections were refined based on F_o by full-matrix least squares. b) Crystal data for **2**: $C_{62}H_{94}O_2N_{26}Ni_2$, $M_r = 1353.00$, orthorhombic, space group $Pca2_1$ (no. 29), $a = 18.667(2)$, $b = 23.7236(8)$, $c = 16.786(1)$ Å, $V = 7433.6(8)$ Å^3, $Z = 4$, $\rho_{calcd} = 1.209$ g cm^{-3}, $F(000) = 2880$, 829 parameters; $R_1 = 0.065$, $R_w = 0.079$, GOF = 1.63 for all 2803 data ($I > 3\sigma(I)$); max./min. residual electron density: 0.44/ – 0.27 e Å^{-3}. Diffractometer: Nonius CAD4; $\mu(Cu_{K\alpha}) = 10.90$ cm^{-1}; Lp correction; 7729 relections collected; the solution was solved with the program SAPI91, and refined with the program DIRDIF94; reflections were refined based on F_o by full-matrix least squares. c) Crystal data for **3**: $C_{41}H_{67}O_{11}N_{12}NiK$, $M_r = 1001.85$, monoclinic, space group $C2/m$ (no. 12), $a = 19.077(3)$, $b = 29.074(3)$, $c = 9.769(3)$, $\beta = 110.39(2)^\circ$, $V = 5078(1)$ Å^3, $Z = 4$, $\rho_{calcd} = 1.310$ g cm^{-3}, $F(000) = 2128$, 287 parameters; $R_1 = 0.057$, $R_w = 0.073$, GOF = 1.77 for all 1484 data ($I > 3\sigma(I)$), max./min. residual electron density 0.29/ – 0.29 e Å^{-3}. Diffractometer: Rigaku AFC7R; $\mu(Cu_{K\alpha}) = 18.38$ cm^{-1}; Lp correction; 4004 reflections collected; the structure was solved with the program PATTY, and refined with the program DIRDIF94; reflections were refined based on F_o by full-matrix least squares. d) Crystal data for **4**: $C_{60}H_{84}O_2N_{30}Ni_2$, $M_r = 1374.92$, tetragonal, space group $P4_12_12$ (no. 92), $a = 19.061(1)$, $c = 38.474(2)$ Å, $V = 13977(1)$ Å^3, $Z = 8$, $\rho_{calcd} = 1.307$ g cm^{-3}, $F(000) = 5808$, 778 parameters; $R_1 = 0.075$, $R_w = 0.109$, GOF = 1.83 for all 3213 data ($I > 3\sigma(I)$), max./min. residual electron density 0.80/ – 0.36 e Å^{-3}. Diffractometer: Rigaku AFC7R; $\mu(Cu_{K\alpha}) = 11.89$ cm^{-1}; Lp correction; 5374 reflections collected; the structure was solved with the program SHLXS86, and refined with the program DIRDIF94; reflections were refined based on F_o by full-matrix least squares.
[13] J. S. Moore, S. Lee, *Chem. Ind.* **1994**, 556 – 560.
[14] L. Carlucci, G. Ciani, D. M. Proserpio, A. Sironi, *J. Am. Chem. Soc.* **1995**, *117*, 4562 – 4569.

Bioaffinity NMR Spectroscopy: Identification of an E-Selectin Antagonist in a Substance Mixture by Transfer NOE**

Dirk Henrichsen, Beat Ernst, John L. Magnani, Wei-Tong Wang, Bernd Meyer,* and Thomas Peters*

Leukocytes play a central role in the body's resistance to tissue lesions and microbial infections. So to be able to exercise their defense function, they must selectively enter the area of the affected tissue. The first step in this inflammatory cascade is the cytokine-induced expression of P-selectin and E-selectin, which, located on the surface of endothelial cells, interact specifically with ligands on leukocyte surfaces. With E-selectin this is the ESL – 1 ligand, with P-selectin the PSGL – 1 ligand.[1] The specific interactions between selectins and ligands first initiate a "rolling" of the leukocytes, which leads to further specific interactions with other membrane proteins and, ultimately, to leukocyte migration into the affected tissue. In pathological situations such as myocardial infarction, transplantation, or rheumatoid arthritis, suppression of the inflammatory cascade is desirable. Considerable effort has therefore been expended on the preparation of potent P- and E-selectin antagonists.[2] In the case of E-selectin, the bioactive conformation of the sialyl Lewis^x mimetic **2** was recently elucidated by transfer NOE experiments.[3] It emerged that the bioactive conformation of this antagonist has much in common with that of the sialyl Lewis^x **1** (see Scheme 1).[4]

As always in the search for active compounds, the search for sialyl Lewis^x mimetics requires screening procedures that allow the rapid identification of lead compounds. A procedure we have described recently, "bioaffinity NMR spectroscopy", is based on the selective detection of transfer NOEs (trNOEs).[5] It makes use of the observation that small molecules (relative molecular mass up to about 2 kDa) exhibit strong negative trNOEs when bound to receptor proteins, and can thus be differentiated from nonbinding molecules with weak positive NOEs. Isotope labeling of the

[*] Prof. Dr. B. Meyer
Institut für Organische Chemie der Universität Hamburg
Martin-Luther-King-Platz 6, D-20146 Hamburg (Germany)
Fax: (+49) 40-4123-2878
E-mail: bernd.meyer@sgi1.chemie.uni-hamburg.de
Prof. Dr. T. Peters, Dipl.-Chem. D. Henrichsen
Institut für Chemie der Medizinischen Universität
Ratzeburger Allee 160, D-23538 Lübeck (Germany)
Fax: (+49) 451-500-4241
E-mail: tp@chemie.mu-luebeck.de
Prof. Dr. B. Ernst[+]
Novartis Pharma AG, Basel (Switzerland)
Dr. J. L. Magnani, Dr. W.-T. Wang
GlycoTech Corp., Rockville, MD (USA)
[+] Present Address:
Universität Basel, Institut für Pharmazie
Basel (Switzerland)

[**] This work was supported by BMBF (FKZ 031161 and 0311395), the Deutschen Forschungsgemeinschaft (Sonderforschungsbereich 470, Teilprojekt B3), and the Fonds der Chemischen Industrie. We thank Dr. T. Keller and Dr. G. Wolff (Bruker Analytik GmbH, Rheinstetten) for excellent support.

  1433-7851/99/3801-0098 $ 17.50+.50/0